CONTRACTED FUNCTIONAL CONNECTIVITY PROFILES IN AUTISM

Clara F. Weber[1,2,3], Valeria Kebets[1], Oualid Benkarim[1], Sara Lariviere[1], Yezhou Wang[1], Alexander Ngo[1], Hongxiu Jiang[1], Xiaoqian Chai[4], Bo-yong Park[5,6], Michael P. Milham[7], Adriana Di Martino[7], Sofie Valk[8], Seok-Jun Hong[6,7,9], Boris C. Bernhardt[1]

[1]*Multimodal Imaging and Connectome Analysis Laboratory, McConnell Imaging Center, Montreal Neurological Institute, McGill University, Montreal, Quebec, Canada*
[2]*Social Neuroscience Lab, Department of Psychiatry and Psychotherapy, University of Lübeck, Lübeck, Germany*
[3]*Center of Brain, Behavior and Metabolism (CBBM), University of Lübeck, Lübeck, Germany*
[4]*Department of Neurology and Neurosurgery, McGill University, Montreal, Quebec, Canada*
[5]*Department of Data Science, Inha University, Incheon, South Korea*
[6]*Center for Neuroscience Imaging Research, Institute for Basic Research, Suwon, South Korea*
[7]*Center for the Developing Brain, Child Mind Institute, New York, USA*
[8]*Cognitive Neurogenetics Group, Max Planck Institute for Human Cognitive and Brain Sciences, Leipzig, Germany*
[9]*Department of Biomedical Engineering, Center for Neuroscience Imaging Research, Institute for Basic Science, Sungkyunkwan University, South Korea*

ABSTRACT (294 words)

Objective. Autism spectrum disorder (ASD) is a pervasive neurodevelopmental condition that is associated with atypical brain network organization, with prior work suggesting differential connectivity alterations with respect to functional connection length. Here, we tested whether functional connectopathy in ASD specifically relates to disruptions in long- relative to short-range functional connectivity profiles. Our approach combined functional connectomics with geodesic distance mapping, and we studied associations to macroscale networks, microarchitectural patterns, as well as socio-demographic and clinical phenotypes.

Methods. We studied 211 males from three sites of the ABIDE-I dataset comprising 103 participants with an ASD diagnosis (mean±SD age=20.8±8.1 years) and 108 neurotypical controls (NT, 19.2±7.2 years). For each participant, we computed cortex-wide connectivity distance (CD) measures by combining geodesic distance mapping with resting-state functional connectivity profiling. We compared CD between ASD and NT participants using surface-based linear models, and studied associations with age, symptom severity, and intelligence scores. We contextualized CD alterations relative to canonical networks and explored spatial associations with functional and microstructural cortical gradients as well as cytoarchitectonic cortical types.

Results. Compared to NT, ASD participants presented with widespread reductions in CD, generally indicating shorter average connection length and thus suggesting reduced long-range connectivity but increased short-range connections. Peak reductions were localized in transmodal systems (*i.e.,* heteromodal and paralimbic regions in the prefrontal, temporal, and parietal and temporo-parieto-occipital cortex), and effect sizes correlated with the sensory-transmodal gradient of brain function. ASD-related CD reductions appeared consistent across inter-individual differences in age and symptom severity, and we observed a positive correlation of CD to IQ scores.

Conclusions. Our study showed reductions in CD as a relatively stable imaging phenotype of ASD that preferentially impacted paralimbic and heteromodal association systems. CD reductions in ASD corroborate previous reports of ASD-related imbalance between short-range overconnectivity and long-range underconnectivity.

INTRODUCTION

Autism spectrum disorder (ASD) is a prevalent and pervasive neurodevelopmental condition [1, 2], commonly manifesting in atypical social cognition and communication, repetitive behaviors and interests, sometimes together with imbalances in affective, sensory, and perceptual processing [2-4]. Despite extensive research, pathomechanisms of ASD remain incompletely understood. Convergent evidence from molecular, histological, and neuroimaging work suggests atypical brain network organization, motivating continued efforts to identify substrates of autism connectopathy [5-10].

By interrogating brain structure and function *in vivo*, magnetic resonance imaging (MRI) lends itself as a window into the human connectome [11, 12]. Resting-state functional MRI (rs-fMRI) [13-16] can probe whole-brain intrinsic functional networks [17-20], both in terms of functionality and spatial layout [21-25]. Moreover, rs-fMRI analysis has become common in the study of typical and atypical neurodevelopment [5, 25, 26], and in identifying substrates of symptom profiles in complex neurodevelopmental conditions such as ASD [25, 27-30]. Across the cortex, there is an important inter-regional variability of functional connection length: patterns of strong local connectivity are typical for unimodal areas, including the somatosensory and visual systems, where fast and efficient local signal transmission is necessary [23, 31]. Contrarily, long-range connections are increasingly found in heteromodal association systems and paralimbic networks, systems that implicate more integrative, cognitive-related processing [31, 32]. While longer connections are metabolically expensive to build and maintain [31, 33], they conversely provide gains in terms of processing flexibility and integrative capacity [23, 31, 32].

Increasing evidence suggests widespread functional connectivity alterations in ASD, generally reporting mosaic patterns of under- and overconnectivity in ASD as compared to neurotypical controls (NT) [5, 34-37]. In individuals with ASD, short- and long-range connectivity is likely affected differently [34, 38]. While underconnectivity is reported at a global level and in transmodal systems, such as the default mode network (DMN) in ASD [5, 35, 39], there is some literature also emphasizing overconnectivity, primarily in unimodal cortical areas and subcortico-cortical networks [9, 35, 40]. It has been hypothesized that ASD is associated with long-range underconnectivity, but short-range overconnectivity [38, 41, 42]. However, as studies report diverging results, existing evidence fails to provide a comprehensive and mechanistic explanation and spatial mapping of ASD-related connectivity alterations. Functional connectivity and distance length are spatially linked, as long- and short-range connections are neither randomly nor evenly distributed across the cortex, but characteristic connection length of a cortical region mirrors its position in the putative cortical hierarchy [31, 32]. Thus, combining functional neuroimaging and topological information can provide further insights into connectivity shifts in ASD. Previous studies have proposed connectivity distance (CD) as a metric that combines functional connectivity with measures of spatial proximity between brain areas [31, 38, 43], notably by calculating geodesic distance along the cortical surface [43, 44]. CD is the average distance to connected nodes of a given vertex, thus capturing functionally relevant connection lengths [31, 43]. In NT populations, CD has been found to increase with distance to primary cortical areas [31], supporting that short-range connections predominate in unimodal regions while long-range connections are increasingly present in transmodal association systems, such as the DMN. Additional evidence has underlined impaired segregation and integration between cortical hierarchies in ASD mirrored in functional neuroimaging [45].

The well-recognized etiological heterogeneity in ASD motivates contextualization of neuroimaging-based phenotypes against established measures of neural organization, to explore potential pathways of susceptibility. Converging evidence hints towards a relationship between CD and cortical microarchitecture [31, 32, 43, 46, 47], notably cellular composition, columnar topography, and lamination of the cortex [46, 48]. Local increases in cell density and smaller pyramidal cells [49-51], suggestive of short-range overconnectivity at the expense of long-range connections, could potentially impact macrolevel connections and circuit function [50, 52]. Neuronal cell size, density, and connection types vary across cortical areas and their modalities, as observed in histological studies as early as in the foundational descriptions of cortical types by Von Economo and Koskinas [53]. The microstructural organization of the cortex is generally thought to correlate with large-scale functional organization, with unimodal regions exhibiting stronger lamination patterns while transmodal systems express reduced laminar differentiation [54]. More recently, analyzing *post mortem* histological reconstructions of the human brain has allowed for additional histological contextualization of imaging findings [55-59]. In particular, the 3D BigBrain dataset has been used to derive gradients of microstructural cortical organization that run from sensory to paralimbic systems [60]. Despite some notable differences [60, 61], this hierarchical axis is in most parts converging with foundational descriptions of the functional cortical hierarchy [23], and decompositions of resting-state functional connectivity [24, 62, 63]. As such, these novel resources set the stage to explore whether connectome contractions in ASD follow microstructural and functional gradients, indicating a connectopathological susceptibility that follows established principles of cortical hierarchical organization.

Considering the mounting evidence of the differential impact of long- *vs* short-range connectivity alterations in ASD, we aimed to investigate CD in individuals with ASD and NT as a possible underpinning of shorter average connection length, *i.e.* contracted connectome profiles in ASD. We leveraged the multi-centric Autism Brain Imaging Data Exchange (ABIDE-I) repository [64] and quantified CD alterations in ASD relative to NT by combining rs-fMRI connectivity analysis with cortex-wide geodesic distance mapping. We contextualized ASD-related CD reductions across functional networks and sensory-transmodal gradients of cortical functional hierarchy [24]. On a microscopic scale, we investigated correlation to histology-derived gradient maps and cortical types, to find a more complete explanatory model for connectome contractions in ASD.

METHODS

Participants

We studied data from the first release of the Autism Brain Imaging Data Exchange (ABIDE) [64], a multi-centric data and imaging collection consortium. Similar to previous work [25, 65, 66], we included imaging and clinical data from three different sites that included data from >=10 ASD and NT respectively, *i.e.*, University of Pittsburgh School of Medicine (PITT), New York University Langone Medical Center (NYU), and University of Utah School of Medicine (USM). ABIDE data has been collected in alignment with local institutional review board frameworks and made publicly available in an anonymized form in accordance with the Health Insurance Portability and Accountability Act (HIPAA) guidelines. ASD individuals were identified in an in-person diagnostic interview using the Autism Diagnostic Observation Schedule (ADOS), and subjects with genetic disorders associated to ASD, or contraindications to scanning such as pregnancy were excluded from the study. NT controls did not have any history of psychiatric

disease. Due to the small number of female participants included in the first ABIDE release [64], we limited our analysis to male individuals. Additionally, we only retained cases with acceptable T1 imaging quality and surface extraction outcomes. After excluding cases with high head motion as described below, we obtained a sample size of n=211 (103/108 ASD/NT). To assess symptom severity, we considered ADOS scores [4], which evaluate three characteristic symptomatic domains of ASD, *i.e.*, communication and language, reciprocal social interactions and restricted/repetitive behaviors. Furthermore, we considered intelligence quotient (IQ) and IQ subscores for verbal and performance IQ as measured by the Wechsler Adult Intelligence Scale [67]. Since previous literature suggests cognitive imbalances, such as high variability between verbal and nonverbal abilities, in ASD [68, 69], we additionally calculated and analyzed the ratio of verbal over nonverbal IQ [70]. Detailed demographic information is provided in **Table 1**.

MRI Acquisition Parameters

Data from all three sites were acquired on 3T Siemens scanners. Acquisition protocols for T1-weighted (T1w) and rs-fMRI were as follows for the three included sites: *(i) NYU.* Data were acquired on Allegra scanner using 3D-TurboFLASH for T1w (repetition time (TR) = 2530 ms; echo time (TE) = 3.25 ms; inversion time (TI) = 1100 ms; flip angle = 7°; matrix = 256 × 256; 1.3 × 1.0 × 1.3 mm^3 voxels) and 2D-echo planar imaging (EPI) for rs-fMRI (TR = 2000ms; TE = 15 ms; flip angle = 90°; matrix = 80 × 80; 180 volumes, 3.0 × 3.0 × 4.0 mm^3 voxels); *(ii) PITT.* Data were acquired on an Allegra scanner using 3D-MPRAGE for T1w (TR = 2100 ms; TE = 3.93 ms; TI = 1000 ms; flip angle = 7°; matrix = 269 × 269; 1.1 × 1.1 × 1.1 mm^3 voxels) and 2D-EPI for rs-fMRI (TR = 1500 ms; TE = 35 ms; flip angle = 70°; matrix = 64 × 64; 200 volumes, 3.1 × 3.1 × 4.0 mm^3 voxels)*; (iii) USM.* Data were acquired on a TrioTim scanner using 3D-MPRAGE for T1w (TR = 2300 ms; TE = 2.91 ms; TI = 900 ms; flip angle = 9°; matrix = 240 × 256; 1.0 × 1.0 × 1.2 mm^3 voxels) and 2D-EPI for rs-fMRI (TR = 2000ms; TE = 28 ms; flip angle = 90°; matrix = 64 × 64; 240 volumes; 3.4 × 3.4 × 3.0 mm^3 voxels).

MRI Processing

a) Structural MRI processing. T1w data were preprocessed using FreeSurfer v5.1 [71-73] (https://surfer.nmr.mgh.harvard.edu), which included bias field correction, intensity normalization, removal of non-brain tissue, and white matter segmentation. For a more accurate gray/white matter separation and extraction of a vertex-based surface, a mesh model was fit onto the white matter volume. Resulting surfaces were subsequently brought into spherical representation to improve alignment to sulco-gyral patterns.

b) Geodesic distance. We calculated geodesic distance as the physical distance of vertices along the pial surface. Specifically, we computed each individual's intra-hemispheric geodesic distance map between all pairs of vertices within each hemisphere, using the HCP Workbench *surface-geodesic-distance* command [74] (https://www.humanconnectome.org/software/workbench-command) and resampled data to Conte69 surface space to obtain 10,242 vertices per hemisphere [75] (https://github.com/Washington-University/HCPpipelines). Additionally, we extracted intracranial volume measures using FreeSurfer v5.1 [76]. Briefly, this approach leverages the registration matrix between an individual image to a standard atlas space to estimate intracranial volume [77, 78].

c) Resting-state fMRI processing. The rs-fMRI data were processed as described previously [45] based on the configurable pipeline for the analysis of connectomes (C-PAC) (https://fcp-indi.github.io/) [79], including slice-time and head motion correction, skull stripping and intensity normalization. Data were corrected for head motion, as well as white matter and cerebrospinal fluid signals using CompCor [80], followed by band-pass filtering (0.01-0.1Hz). Both T1w and rs-fMRI data were linearly co-registered and mapped to MNI152 space. Functional imaging data were mapped to corresponding mid-thickness surfaces. We resampled data to the Conte69 surface template [75] via Workbench [74] with 10,242 surface points (vertices) per hemisphere. Due to the ongoing debate about global signal regression (GSR) [81], we did not apply GSR, but conducted additional control analyses using data that underwent GSR. We smoothed timeseries using a 5 mm full-width-at-half-maximum Gaussian kernel and computed intra-hemispheric functional connectivity (FC) as the Pearson correlation between all pairs of vertices within each hemisphere. FC matrices were Fisher r-to-z-transformed, to render correlation coefficients more normally distributed. Subjects with a mean framewise displacement (FD) >0.3 mm in rs-fMRI (two SD from the mean across all subjects) were excluded (n=9). Data were harmonized for site effects while preserving effects of age and ASD diagnosis using ComBat [82], which minimizes site-specific scaling factors by estimating their additive and multiplicative influence in a linear model, using empirical Bayes to predict site parameters more accurately [83, 84].

d) Connectivity distance profiling. We integrated FC and geodesic distance measures to compute CD profiles, as described previously [25, 43, 44]. Each participant's functional connectivity matrix was masked to only consider the 10% strongest (*i.e.,* highest absolute) values in each hemisphere. This threshold was chosen as prior literature suggested potential bias towards inter-individual differences with stricter cutoffs, and corresponding loss of functional specificity with more lenient thresholds [31]. Previous literature applying similar methodology applied a similar cutoff [43, 44]. CD was computed by binarizing thresholded functional connectivity matrices and retrieving the row-wise average geodesic distance in these nodes, generating a single value per vertex for each participant. The resulting CD maps, thus, reflects the average distance on the cortex from each region to the areas to which it is strongly connected to, thereby combining anatomical and functional information.

Statistical analysis

We fit surface-based linear models correcting for age and head motion (as measured by mean framewise displacement) at each vertex *i*.

$$CD_i = \beta_0 + \beta_1 * Age + \beta_2 * Diagnosis + \beta_3 * Head\ Motion$$

and group differences between ASD and NT were assessed in vertex-wise two-tailed Student's t-tests using the BrainStat toolbox (https://github.com/MICA-MNI/BrainStat) [56]. Additionally, we computed vertex-wise effect sizes using *Cohen's d***.** Resulting p-values were adjusted for multiple comparisons using random field theory correction [85].

Several *post-hoc* analyses investigated the relationship between CD and behavioral metrics. Within ASD, we tested for associations to ASD symptom severity scores, specifically, total ADOS scores and ADOS subscores for communication, social interaction, and repetitive behaviors. In both ASD and NT groups, we examined the correlation to total IQ as well as verbal and performance IQ subscores, and the ratio of verbal and performance IQ [70]. First, we assessed the

whole-brain association of CD with behavioral metrics in a vertex-wise linear model as described above. Additionally, we assessed the association to behavioral metrics within clusters of significant group differences which were identified in the previous step. Mean CD values were extracted from each cluster and the correlation to IQ and ADOS metrics were determined, adjusting for multiple comparisons using a false discovery rate (FDR) correction method [86].

Contextualization to macro- and microscale principles of cortical organization

We explored effect sizes for group differences between ASD and NT individuals, *i.e.* Cohen's *d*-values, and studied associations to macro- and microscale cortical patterns. For the whole-brain large-scale investigation, we analyzed mean CD and effect sizes in each of the seven previously described intrinsic functional networks [21]. Subsequently, we assessed the spatial correlation between Cohen's *d* effect sizes and scores of the principal functional gradient that describes sensory-transmodal functional differentiation [24], while accounting for spatial autocorrelation with 5000 spin permutations [87]. We similarly investigated effect sizes within cytoarchitectonic cortical types of Von Economo and Koskinas [53, 54] leveraging the ENIGMA toolbox [57]. Finally, we assessed associations to the BigBrain histology gradient that describes microstructural differentiation [88], again sourced from the ENIGMA toolbox [57].

RESULTS

Reduced connectivity distance (CD) in autism

Mean CD in NT was higher within transmodal regions (*i.e.,* heteromodal and paralimbic regions), such as the prefrontal and cingulate cortex and temporo-occipital-parietal junction, while CD values were lower in primary sensory and motor regions (**Figure 1A**).

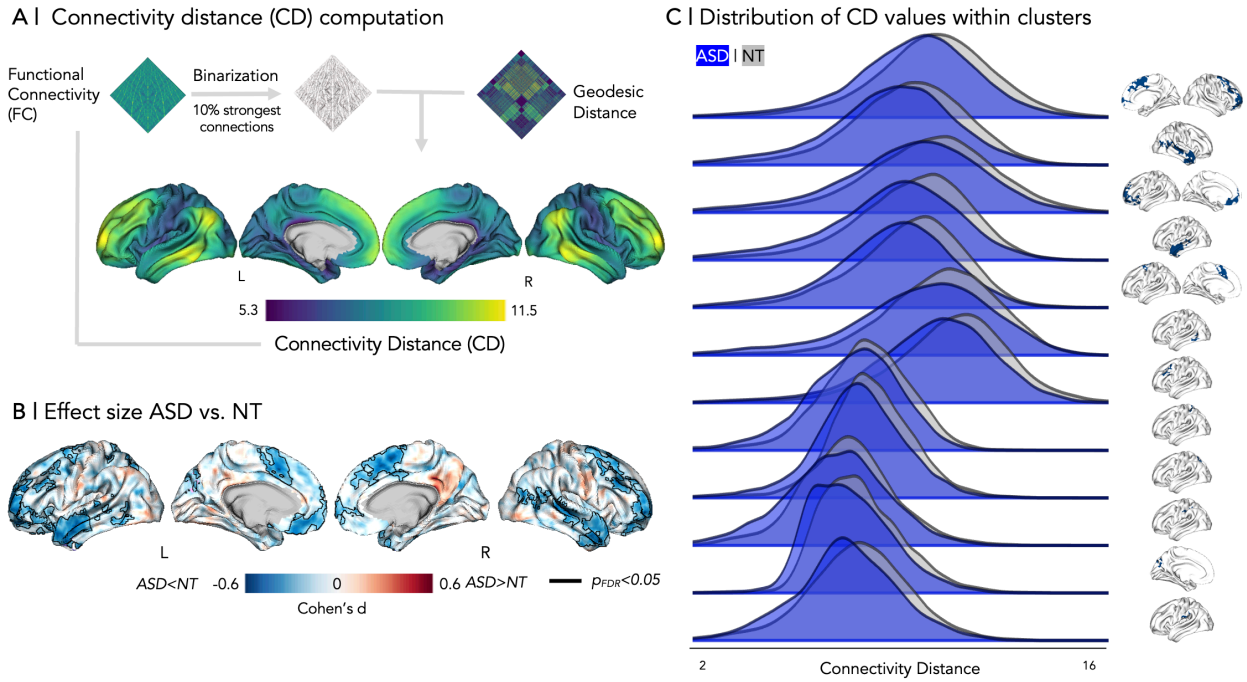

FIGURE 1. A | Workflow for CD computation and average CD maps. **B** | Effect size map for group differences (ASD *vs* NT). Clusters of significant changes after multiple comparisons correction are outlined (p_{FDR}<0.05, vertex-based linear model). **C** | Distribution of CD values within clusters of significant reduction.

Comparing groups with linear models that additionally corrected for age and head motion revealed diffuse CD reductions in ASD relative to NT (**Figure 1B**), with twelve clusters deemed significant after multiple comparisons correction (p_{RFT}<0.05). Clusters were mainly localized in the left and right temporal lobes and left prefrontal cortex (**Figure 1B, 2A**). *Cohen's d* effect sizes for between-group differences amounted to d=0.600 in the temporal lobes as well as in the left prefrontal cortex (**Figure 1B**). Overall, there was a consistent shift of the CD distributions in ASD relative to NT across all significant clusters **(Figure 1C)**. Of note, CD was averaged per vertex, hence, the apparent decrease mirrors an increase in short-range connections at the expense of long-range links [43].

Effects of age, symptom severity and intelligence measures

Within clusters of significant ASD-related reductions identified in the vertex-wise model, there was no significant correlation to age (r=0.151, p_{FDR}=0.274**, Table 2)**. Moreover, there were no between-group effects when comparing children and adults, which indicated that ASD-related CD reductions were stable across pediatric and adult cohorts (t=-0.469, p_{FDR}=0.640, **Figure 2B, Table 2**).

Within clusters of significant between-group differences, CD in the ASD group also did not show any significant associations with ADOS symptom severity scores (r=0.047, p_{FDR}>0.4) nor with subscores for communication (r=0.028, p_{FDR}>0.4), social interaction (r=0.049, p_{FDR}=>0.4), and repetitive behaviors and interests (r=-0.037, p_{FDR}>0.4). On the other hand, when averaged within

all clusters, there was a significant association of CD with full (r=0.324, p_{FDR}<0.001), verbal (r=0.304, p_{FDR}<0.001), and performance IQ (r=0.245, p_{FDR}=0.001; **Table 2**), while no significant interaction between diagnosis group and IQ measures was detectable (full IQ: r=-0.004, p_{FDR}=0.561, verbal IQ: r=0.005, p_{FDR}=0.561, performance IQ: r=-0.011, p_{FDR}=0.214, IQ ratio: r=1.476, p_{FDR}=0.128). Similar results were obtained in cluster-wise analysis. **Figure 2C-D** shows correlation between behavioral metrics and mean CD across all clusters, while separate cluster-wise analyses can be found in **Supplemental Figure 2 & Supplemental Table 1**.

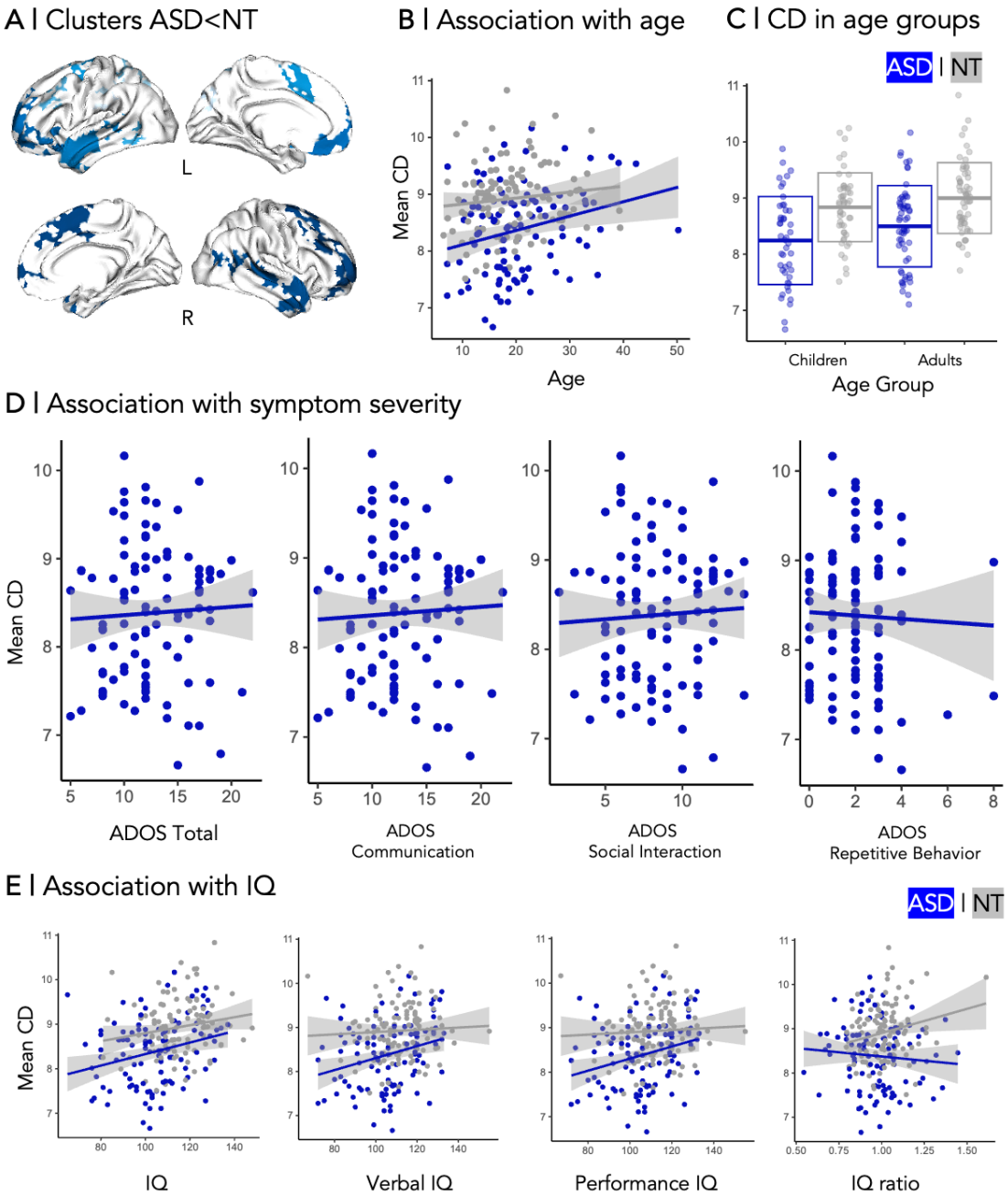

FIGURE 2: A | Clusters of significant CD reduction in ASD *vs* NT. **B-E |** Correlation between mean CD in clusters and age, age group (children <18 years, adults >18 years), total ADOS score, ADOS subscores for communication, social

interaction, and repetitive behavior, as well as full IQ and IQ subscores for verbal and nonverbal IQ. IQ ratio denotes the ratio of verbal over nonverbal IQ. Correlation coefficients are listed in **Table 2**.

In addition to cluster-wise analyses, we assessed whole-brain associations between CD and clinical metrics using a linear model of the influence of a behavioral score on CD while accounting for head motion and age. Overall, vertex-wise findings were consistent with within-cluster results (**Supplemental Figure 3**).

Relation to cortical organization

Macroscale functional contextualization. Effect sizes differed across seven intrinsic functional networks [21], with higher effects towards transmodal compared to sensory/motor networks and peak reductions in CD in the limbic network (*Cohen's d*=-0.159, **Figure 3A**). These findings were recapitulated when correlating effects against the intrinsic functional gradient [24] (r=-0.381, p_{spin}<0.001), which were significant even when using models correcting for spatial autocorrelation (**Figure 3B**).

Microstructural and cytoarchitectonic contextualization. For cortical types as proposed by Von Economo and Koskinas [54], we were able to see notable effect size variations that also became larger towards limbic/paralimbic regions, with highest effect sizes being present in agranular polar cortex (*Cohen's d*=0.201, **Figure 3C**). On the other hand, there was only a weak correlation between effects sizes and the primary BigBrain microstructural gradient (r=-0.148, p_{spin}=0.265; **Figure 3D**).

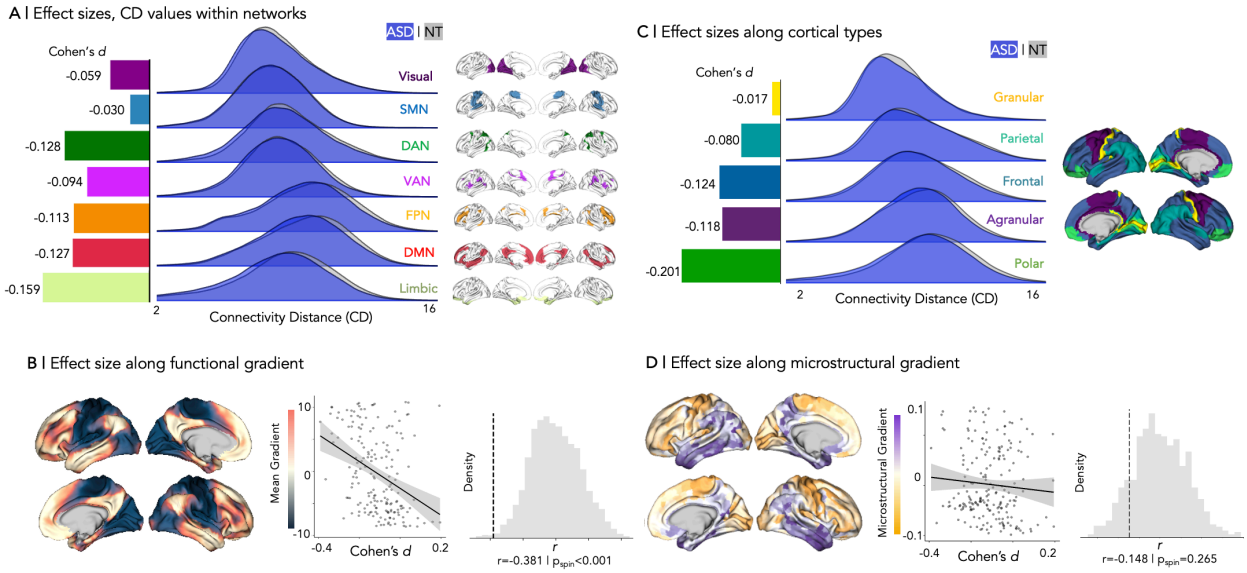

Figure 3. Relation to cortical organization. **A |** Effect sizes of between-group differences (ASD *vs* NT) in functional CD measures, stratified within seven intrinsic networks proposed by Yeo, Krienen, *et al.* [21] **B** | Correlation to the principal functional gradient [24]. Spatial associations were assessed using Spearman's rank test, and p-values were adjusted for spatial autocorrelation using a spin test [87, 89]. **C** | Effect size for the between-group difference in functional CD in each cortical type as proposed by Von Economo and Koskinas [54]. **D** | Association to microstructural gradients derived from the 3D BigBrain [55]. *Abbreviations:* SMN = somatomotor network, DAN =

dorsal attention network, VAN = ventral attention network, FPN = frontoparietal network, DMN= default mode network.

Control analyses

To ensure the robustness of our results across different data processing methods, we repeated analyses using functional connectivity that underwent GSR. **Supplemental Figure 2** shows respective effect size maps for both CD differences from uncorrected and from GSR-corrected functional CD maps. In both contrasts, highest between-group differences were localized in the left temporal lobe and left prefrontal cortex, as well as the right frontal lobe. However, group differences appeared higher for uncorrected data in medial prefrontal regions bilaterally, as well as the right temporal lobe. The congruence of both maps (r=0.546, p<0.001) suggested robustness of our results with respect to GSR application *vs* omission during data preprocessing. Additionally, we assessed intracranial volume as a potential confound for geodesic distance measures. There was no significant between-group difference in intracranial volume (t=0.694, p=0.488). Of note, there were eminent site-related differences in ADOS scores, suggesting behavioral phenotype differences between the cohorts or variations in clinical symptom severity assessment (F=3.904, p=0.023, **Supplemental Figure 4**).

DISCUSSION

Atypical brain connectivity is thought to be at the core of autism [90] and our study examined whether ASD implicates long-range underconnectivity and local overconnectivity as compared to NT. We combined functional connectivity analysis with cortex-wide geodesic distance mapping and characterized overall shifts in the spatial extent of regional connectivity profiles [25, 43, 44]. Leveraging the open-access ABIDE dataset composed of ASD and NT individuals, we found robust evidence for global CD reductions in ASD, hinting towards a deficiency in long-range connections and a compensatory increase in short-range connectivity. Examining associations to functional topography, we noted a significant correlation to sensory-transmodal functional gradients, with most marked findings in paralimbic and heteromodal functional zones [24]. Likewise, contextualization against cytoarchitectural taxonomy [53, 54, 57] revealed most marked effects in agranular and polar cortices with low laminar differentiation. Findings were relatively robust irrespective of using GSR during preprocessing and were consistent across the different sites and age strata included in the study. Furthermore, CD reductions were stable across symptom severity metrics. While our findings did, thus, not capture imaging correlates of inter-individual differences in autism symptom load, they constitute a stable imaging phenotype of the condition. Moreover, CD alterations were positively correlated to both verbal and performance IQ measures, suggesting that these imbalances may index overall cognitive function in ASD. Collectively, imbalances in connectivity length distribution constitute a stable imaging phenotype of atypical neurodevelopment in ASD, representing a gradient of susceptibility closely intertwined with overarching principles of cortical organization.

The CD measure employed in this work combined rs-fMRI as an established *in vivo* proxy for functional interactions [91] with cortex-wide geodesic distance mapping [24, 43, 92, 93] to profile average functional connection length. This metric has been suggested to mirror functional and hierarchical properties of cortical areas, and to stratify systems in a data-driven, yet anatomically meaningful way [31, 32]. Prior research and our current findings have consistently demonstrated that long-range cortico-cortical connections predominate in transmodal networks, which comprise

heteromodal association systems such as the DMN as well as paralimbic cortices [26, 39, 45]. These connections ensure efficient integration of functional signals in higher-order networks that are increasingly involved in abstract, integrative, as well as internally-generated cognitive and affective processes [16, 24, 94]. The observed decrease in long-range connectivity in ASD in this study may indicate brain reorganization characterized by reduced inter-network connectivity together with compensatory strengthening of local connections [41]. The topography of CD changes in ASD may indeed be particularly meaningful in the context of cortical hierarchies, a conjecture supported by the macro- and microscale contextualization analyses conducted in the current work. Here, we observed a sensory-fugal pattern of ASD-related CD alterations when cross-referencing our findings to both intrinsic functional and microstructural measures. Specifically, we observed that ASD-related CD alterations mirrored the intrinsic functional gradient of information abstraction, which runs from primary input to unimodal regions to higher-level cognition in transmodal cortices [30, 45]. Stratifying findings across seven intrinsic networks derived in previous work [21], we also found the largest effect sizes in limbic networks, confirming that ASD-related CD alterations primarily affect paralimbic/fugal systems. The latter conclusion could be supported by cross-referencing ASD-related effects to microstructure-based neural data. In fact, cytoarchitecture type stratification of our *in vivo* imaging-derived metrics revealed the strongest effect sizes in limbic agranular and polar cortices [53].

Our findings demonstrated increased vulnerability for ASD-associated connection length contractions in heteromodal and paralimbic cortices that collectively make up the transmodal core of cortical organization [62, 95-97]. When considering anatomical but also functional connectivity relationships across the cortex, both paralimbic as well as heteromodal association cortices are situated at a high distance from primary sensory and motor regions interacting with the here and now [98, 99]. When considering cortical microarchitecture, particularly its laminar organization, there has been evidence for an axis that differentiates sensory/motor on the one end from paralimbic systems on the other end [58, 60, 100, 101]. These characteristics are highlighted in spatial variations in the visibility of the internal granular layer, commonly referred to as layer IV [98, 102, 103]. In effect, the agranular cortex lacks the respective layer, the dysgranular cortex exhibits rudimentary layer IV characteristics, and the granular cortex shows clear layer IV [98]. Limbic and paralimbic cortical systems comprise mainly the agranular and dysgranular extent of this spectrum [98, 99, 104]. As such, paralimbic systems are microstructurally most segregated from granular systems interacting with the external environment [60]. Converging, but also somewhat different from the microstructural gradient is the sensory-association functional gradient, which radiates from sensory and motor systems towards heteromodal areas in the DMN [24, 60, 100]. These regions may contain complex microstructural signatures, including agranular types as well as granular cortices [23, 53, 54, 95]. In both heteromodal association systems as well as paralimbic cortices, there is prior evidence to suggest increased susceptibility to neurodevelopmental perturbations [58, 98]. Deficiency in long-range connectivity potentially results from cellular and laminar alterations [43], which may present a common substrate for different psychiatric and neurodevelopmental conditions [47, 58]. Risk genes for ASD as well as other neurodevelopmental conditions impact corticogenesis as early as in germinal stages [105, 106], impacting later axonal development that may disproportionally affect heteromodal systems [50, 107]. In future work, it remains thus to be established whether the current findings are specific to autism, or also visible in related neurodevelopmental indications. Our results, nevertheless, provide further justification to study microcircuit and macroscale alterations based on compact intermediary phenotypes such as CD. As such, they establish a perspective for future research, in

order to better investigate and ultimately understand differentially impacted cortical hierarchies across common neurodevelopmental conditions.

Neuroimaging correlates of the typically developing connectome indicate marked shifts from local towards more distributed network patterns connections, while facilitating signaling across lobes and hemispheres [108, 109]. This progression highlights increased functional integration across brain networks, with short-range connections undergoing functional refinement [110, 111]. As such, network characteristics change from emphasized local processing in children to spatially and functionally distributed effects [109, 111, 112]. A potential microscale developmental mechanism driving this redistribution in typical development may be synaptic pruning [113-116]. In addition to its role in healthy brain maturation [117, 118], atypical pruning has been suggested in ASD [113, 119-121]. In effect, these alterations may be associated with local overconnectivity while not ensuring reliable long-range information relay [113, 119]. While speculative, our results potentially suggest a differential impact of pruning between long- and short-range connections, specifically, a higher requirement for longer connections to be retained in autism.

CD reductions identified in our work were invariant to age or symptom severity, possibly constituting a relatively stable marker of ASD-associated connectome reorganization. On the other hand, CD changes were modulated by intelligence measures, specifically, they exhibited an inverse correlation to IQ. Thus, our findings point towards contracted connectome profiles as markers for overall impaired cognitive performance. Conceptually, connectome contractions as imaged by CD implicate decreased communication efficiency [32, 43], offering a potential explanation for their potential contribution to general cognitive function in atypical development. Further research is needed to confirm this association in larger samples, and to also examine the specificity of these brain-behavior associations for autism *vis-à-vis* other neurodevelopmental indications.

REFERENCES

[1] M. J. Maenner *et al.*, "Prevalence of Autism Spectrum Disorder Among Children Aged 8 Years — Autism and Developmental Disabilities Monitoring Network, 11 Sites, United States, 2016," *MMWR. Surveillance Summaries,* vol. 69, no. 4, pp. 1-12, 2020-03-27 2020, doi: 10.15585/mmwr.ss6904a1.

[2] "American Psychiatric Association", "Diagnostic and Statistical Manual of Mental Disorders (DSM-5®)," ed, 2013.

[3] S. E. Levy, D. S. Mandell, and R. T. Schultz, "Autism," *The Lancet,* vol. 374, no. 9701, pp. 1627-1638, 2009-11-01 2009, doi: 10.1016/s0140-6736(09)61376-3.

[4] C. Lord *et al.*, "The Autism Diagnostic Observation Schedule-Generic: A standard measure of social and communication deficits associated with the spectrum of autism," vol. 30, ed: Springer, 2000, pp. 205-223.

[5] M. Assaf *et al.*, "Abnormal functional connectivity of default mode sub-networks in autism spectrum disorder patients," *Neuroimage,* vol. 53, no. 1, pp. 247-56, Oct 15 2010, doi: 10.1016/j.neuroimage.2010.05.067.

[6] S. H. Ameis and M. Catani, "Altered white matter connectivity as a neural substrate for social impairment in Autism Spectrum Disorder," vol. 62, ed: Masson SpA, 2015, pp. 158-181.

[7] W. Sato and S. Uono, "The atypical social brain network in autism: Advances in structural and functional MRI studies," vol. 32, ed: Lippincott Williams and Wilkins, 2019, pp. 617-621.

[8] S. J. Hong *et al.*, "Toward Neurosubtypes in Autism," *Biol Psychiatry,* vol. 88, no. 1, pp. 111-128, Jul 1 2020, doi: 10.1016/j.biopsych.2020.03.022.

[9] E. Delbruck, M. Yang, A. Yassine, and E. D. Grossman, "Functional connectivity in ASD: Atypical pathways in brain networks supporting action observation and joint attention," *Brain Res,* vol. 1706, pp. 157-165, Mar 1 2019, doi: 10.1016/j.brainres.2018.10.029.

[10] M. L. Simms, T. L. Kemper, C. M. Timbie, M. L. Bauman, and G. J. Blatt, "The anterior cingulate cortex in autism: heterogeneity of qualitative and quantitative cytoarchitectonic features suggests possible subgroups," *Acta Neuropathol,* vol. 118, no. 5, pp. 673-84, Nov 2009, doi: 10.1007/s00401-009-0568-2.

[11] P. Rane, D. Cochran, S. M. Hodge, C. Haselgrove, D. N. Kennedy, and J. A. Frazier, "Connectivity in Autism: A Review of MRI Connectivity Studies," vol. 23, ed: Taylor and Francis Ltd, 2015, pp. 223-244.

[12] J. V. Hull, L. B. Dokovna, Z. J. Jacokes, C. M. Torgerson, A. Irimia, and J. D. Van Horn, "Resting-State Functional Connectivity in Autism Spectrum Disorders: A Review," *Front Psychiatry,* vol. 7, p. 205, 2016, doi: 10.3389/fpsyt.2016.00205.

[13] G. H. Glover, "Overview of functional magnetic resonance imaging," *Neurosurg Clin N Am,* vol. 22, no. 2, pp. 133-9, vii, Apr 2011, doi: 10.1016/j.nec.2010.11.001.

[14] M. D. Fox and M. E. Raichle, "Spontaneous fluctuations in brain activity observed with functional magnetic resonance imaging," *Nature Reviews Neuroscience,* vol. 8, no. 9, pp. 700-711, 2007-09-01 2007, doi: 10.1038/nrn2201.

[15] D. A. Gusnard, M. E. Raichle, and M. E. Raichle, "Searching for a baseline: functional imaging and the resting human brain," *Nat Rev Neurosci,* vol. 2, no. 10, pp. 685-94, Oct 2001, doi: 10.1038/35094500.

[16] M. D. Greicius, B. Krasnow, A. L. Reiss, and V. Menon, "Functional connectivity in the resting brain: a network analysis of the default mode hypothesis," *Proc Natl Acad Sci U S A,* vol. 100, no. 1, pp. 253-8, Jan 7 2003, doi: 10.1073/pnas.0135058100.

[17] M. D. Fox, A. Z. Snyder, J. L. Vincent, M. Corbetta, D. C. Van Essen, and M. E. Raichle, "The human brain is intrinsically organized into dynamic, anticorrelated functional networks," *Proc Natl Acad Sci U S A,* vol. 102, no. 27, pp. 9673-8, Jul 5 2005, doi: 10.1073/pnas.0504136102.

[18] D. M. Barch *et al.*, "Function in the human connectome: task-fMRI and individual differences in behavior," *Neuroimage,* vol. 80, pp. 169-89, Oct 15 2013, doi: 10.1016/j.neuroimage.2013.05.033.

[19] E. S. Finn *et al.*, "Functional connectome fingerprinting: identifying individuals using patterns of brain connectivity," *Nat Neurosci,* vol. 18, no. 11, pp. 1664-71, Nov 2015, doi: 10.1038/nn.4135.

[20] J. S. Damoiseaux *et al.*, "Consistent resting-state networks across healthy subjects," *Proc Natl Acad Sci U S A,* vol. 103, no. 37, pp. 13848-53, Sep 12 2006, doi: 10.1073/pnas.0601417103.

[21] B. T. Yeo *et al.*, "The organization of the human cerebral cortex estimated by intrinsic functional connectivity," *J Neurophysiol,* vol. 106, no. 3, pp. 1125-65, Sep 2011, doi: 10.1152/jn.00338.2011.

[22] S. M. Smith *et al.*, "Correspondence of the brain's functional architecture during activation and rest," *Proc Natl Acad Sci U S A,* vol. 106, no. 31, pp. 13040-5, Aug 4 2009, doi: 10.1073/pnas.0905267106.

[23] M. M. Mesulam, "From sensation to cognition," *Brain,* vol. 121 (Pt 6), pp. 1013-52, Jun 1998, doi: 10.1093/brain/121.6.1013.

[24] D. S. Margulies *et al.*, "Situating the default-mode network along a principal gradient of macroscale cortical organization," *Proc Natl Acad Sci U S A,* vol. 113, no. 44, pp. 12574-12579, Nov 1 2016, doi: 10.1073/pnas.1608282113.

[25] S.-J. Hong *et al.*, "Atypical functional connectome hierarchy in autism," *Nature Communications,* vol. 10, no. 1, 2019-12-01 2019, doi: 10.1038/s41467-019-08944-1.

[26] Y. Funakoshi, M. Harada, H. Otsuka, K. Mori, H. Ito, and T. Iwanaga, "Default mode network abnormalities in children with autism spectrum disorder detected by resting-state functional magnetic resonance imaging," *J Med Invest,* vol. 63, no. 3-4, pp. 204-8, 2016, doi: 10.2152/jmi.63.204.

[27] C. Sripada, D. Kessler, Y. Fang, R. C. Welsh, K. Prem Kumar, and M. Angstadt, "Disrupted network architecture of the resting brain in attention-deficit/hyperactivity disorder," *Hum Brain Mapp,* vol. 35, no. 9, pp. 4693-705, Sep 2014, doi: 10.1002/hbm.22504.

[28] K. Konrad and S. B. Eickhoff, "Is the ADHD brain wired differently? A review on structural and functional connectivity in attention deficit hyperactivity disorder," *Hum Brain Mapp,* vol. 31, no. 6, pp. 904-16, Jun 2010, doi: 10.1002/hbm.21058.

[29] O. Benkarim *et al.*, "Connectivity alterations in autism reflect functional idiosyncrasy," *Commun Biol,* vol. 4, no. 1, p. 1078, Sep 15 2021, doi: 10.1038/s42003-021-02572-6.

[30] S.-J. Hong *et al.*, "Toward Neurosubtypes in Autism," vol. 88, ed, 2020, pp. 111-128.

[31] S. Oligschläger, J. M. Huntenburg, J. Golchert, M. E. Lauckner, T. Bonnen, and D. S. Margulies, "Gradients of connectivity distance are anchored in primary cortex," *Brain*

Structure and Function, vol. 222, no. 5, pp. 2173-2182, 2017-07-01 2017, doi: 10.1007/s00429-016-1333-7.

[32] S. Oligschläger *et al.*, "Gradients of connectivity distance in the cerebral cortex of the macaque monkey," *Brain Structure and Function,* vol. 224, no. 2, pp. 925-935, 2019-03-01 2019, doi: 10.1007/s00429-018-1811-1.

[33] P. Somogyi, G. Tamas, R. Lujan, and E. H. Buhl, "Salient features of synaptic organisation in the cerebral cortex," *Brain Res Brain Res Rev,* vol. 26, no. 2-3, pp. 113-35, May 1998, doi: 10.1016/s0165-0173(97)00061-1.

[34] R. A. Muller, P. Shih, B. Keehn, J. R. Deyoe, K. M. Leyden, and D. K. Shukla, "Underconnected, but how? A survey of functional connectivity MRI studies in autism spectrum disorders," *Cereb Cortex,* vol. 21, no. 10, pp. 2233-43, Oct 2011, doi: 10.1093/cercor/bhq296.

[35] K. Supekar *et al.*, "Brain hyperconnectivity in children with autism and its links to social deficits," *Cell Rep,* vol. 5, no. 3, pp. 738-47, Nov 14 2013, doi: 10.1016/j.celrep.2013.10.001.

[36] M. A. Just, V. L. Cherkassky, T. A. Keller, R. K. Kana, and N. J. Minshew, "Functional and anatomical cortical underconnectivity in autism: evidence from an FMRI study of an executive function task and corpus callosum morphometry," *Cereb Cortex,* vol. 17, no. 4, pp. 951-61, Apr 2007, doi: 10.1093/cercor/bhl006.

[37] M. A. Just, T. A. Keller, V. L. Malave, R. K. Kana, and S. Varma, "Autism as a neural systems disorder: a theory of frontal-posterior underconnectivity," *Neurosci Biobehav Rev,* vol. 36, no. 4, pp. 1292-313, Apr 2012, doi: 10.1016/j.neubiorev.2012.02.007.

[38] Z. Long, X. Duan, D. Mantini, and H. Chen, "Alteration of functional connectivity in autism spectrum disorder: effect of age and anatomical distance," *Scientific Reports,* vol. 6, no. 1, p. 26527, 2016-05-01 2016, doi: 10.1038/srep26527.

[39] E. A. von dem Hagen, R. S. Stoyanova, S. Baron-Cohen, and A. J. Calder, "Reduced functional connectivity within and between 'social' resting state networks in autism spectrum conditions," *Soc Cogn Affect Neurosci,* vol. 8, no. 6, pp. 694-701, Aug 2013, doi: 10.1093/scan/nss053.

[40] L. Cerliani, M. Mennes, R. M. Thomas, A. Di Martino, M. Thioux, and C. Keysers, "Increased Functional Connectivity Between Subcortical and Cortical Resting-State Networks in Autism Spectrum Disorder," *JAMA Psychiatry,* vol. 72, no. 8, pp. 767-77, Aug 2015, doi: 10.1001/jamapsychiatry.2015.0101.

[41] H. Haghighat, M. Mirzarezaee, B. N. Araabi, and A. Khadem, "Functional Networks Abnormalities in Autism Spectrum Disorder: Age-Related Hypo and Hyper Connectivity," *Brain Topogr,* vol. 34, no. 3, pp. 306-322, May 2021, doi: 10.1007/s10548-021-00831-7.

[42] E. Courchesne and K. Pierce, "Why the frontal cortex in autism might be talking only to itself: local over-connectivity but long-distance disconnection," *Curr Opin Neurobiol,* vol. 15, no. 2, pp. 225-30, Apr 2005, doi: 10.1016/j.conb.2005.03.001.

[43] Y. Wang *et al.*, "Long-range functional connections mirror and link microarchitectural and cognitive hierarchies in the human brain," *Cereb Cortex,* May 22 2022, doi: 10.1093/cercor/bhac172.

[44] S. Larivière *et al.*, "Functional connectome contractions in temporal lobe epilepsy: Microstructural underpinnings and predictors of surgical outcome," *Epilepsia,* vol. 61, no. 6, pp. 1221-1233, 2020-06-01 2020, doi: 10.1111/epi.16540.

[45] S. J. Hong *et al.*, "Atypical functional connectome hierarchy in autism," *Nat Commun,* vol. 10, no. 1, p. 1022, Mar 4 2019, doi: 10.1038/s41467-019-08944-1.

[46] D. Arion, T. Unger, D. A. Lewis, and K. Mirnics, "Molecular markers distinguishing supragranular and infragranular layers in the human prefrontal cortex," *Eur J Neurosci,* vol. 25, no. 6, pp. 1843-54, Mar 2007, doi: 10.1111/j.1460-9568.2007.05396.x.

[47] D. Arion, S. Horvath, D. A. Lewis, and K. Mirnics, "Infragranular gene expression disturbances in the prefrontal cortex in schizophrenia: signature of altered neural development?," *Neurobiol Dis,* vol. 37, no. 3, pp. 738-46, Mar 2010, doi: 10.1016/j.nbd.2009.12.013.

[48] H. J. Kang *et al.*, "Spatio-temporal transcriptome of the human brain," *Nature,* vol. 478, no. 7370, pp. 483-9, Oct 26 2011, doi: 10.1038/nature10523.

[49] M. F. Casanova, A. El-Baz, E. Vanbogaert, P. Narahari, and A. Switala, "A topographic study of minicolumnar core width by lamina comparison between autistic subjects and controls: possible minicolumnar disruption due to an anatomical element in-common to multiple laminae," *Brain Pathol,* vol. 20, no. 2, pp. 451-8, Mar 2010, doi: 10.1111/j.1750-3639.2009.00319.x.

[50] J. J. Hutsler and M. F. Casanova, "Review: Cortical construction in autism spectrum disorder: columns, connectivity and the subplate," *Neuropathol Appl Neurobiol,* vol. 42, no. 2, pp. 115-34, Feb 2016, doi: 10.1111/nan.12227.

[51] S. Jacot-Descombes *et al.*, "Decreased pyramidal neuron size in Brodmann areas 44 and 45 in patients with autism," *Acta Neuropathol,* vol. 124, no. 1, pp. 67-79, Jul 2012, doi: 10.1007/s00401-012-0976-6.

[52] M. F. Casanova *et al.*, "Minicolumnar abnormalities in autism," *Acta Neuropathol,* vol. 112, no. 3, pp. 287-303, Sep 2006, doi: 10.1007/s00401-006-0085-5.

[53] C. von Economo and G. N. Koskinas, *Die Cytoarchitektonik der Hirnrinde des erwachsenen Menschen*. Vienna and Berlin: Julius Springer, 1925.

[54] L. C. Triarhou, "The Economo-Koskinas atlas revisited: cytoarchitectonics and functional context," *Stereotact Funct Neurosurg,* vol. 85, no. 5, pp. 195-203, 2007, doi: 10.1159/000103258.

[55] K. Amunts *et al.*, "BigBrain: an ultrahigh-resolution 3D human brain model," *Science,* vol. 340, no. 6139, pp. 1472-5, Jun 21 2013, doi: 10.1126/science.1235381.

[56] S. Lariviere *et al.*, "BrainStat: A toolbox for brain-wide statistics and multimodal feature associations," *Neuroimage,* vol. 266, p. 119807, Feb 1 2023, doi: 10.1016/j.neuroimage.2022.119807.

[57] S. Lariviere *et al.*, "The ENIGMA Toolbox: multiscale neural contextualization of multisite neuroimaging datasets," *Nat Methods,* vol. 18, no. 7, pp. 698-700, Jul 2021, doi: 10.1038/s41592-021-01186-4.

[58] B. Y. Park *et al.*, "Multiscale neural gradients reflect transdiagnostic effects of major psychiatric conditions on cortical morphology," *Commun Biol,* vol. 5, no. 1, p. 1024, Sep 27 2022, doi: 10.1038/s42003-022-03963-z.

[59] C. Paquola *et al.*, "The BigBrainWarp toolbox for integration of BigBrain 3D histology with multimodal neuroimaging," *Elife,* vol. 10, Aug 25 2021, doi: 10.7554/eLife.70119.

[60] C. Paquola *et al.*, "Microstructural and functional gradients are increasingly dissociated in transmodal cortices," *PLoS Biol,* vol. 17, no. 5, p. e3000284, May 2019, doi: 10.1371/journal.pbio.3000284.

[61] Y. Yang *et al.*, "Enhanced brain structure-function tethering in transmodal cortex revealed by high-frequency eigenmodes," *Nat Commun,* vol. 14, no. 1, p. 6744, Oct 24 2023, doi: 10.1038/s41467-023-42053-4.

[62] V. J. Sydnor *et al.*, "Neurodevelopment of the association cortices: Patterns, mechanisms, and implications for psychopathology," *Neuron,* vol. 109, no. 18, pp. 2820-2846, Sep 15 2021, doi: 10.1016/j.neuron.2021.06.016.

[63] Y. Katsumi *et al.*, "Correspondence of functional connectivity gradients across human isocortex, cerebellum, and hippocampus," *Commun Biol,* vol. 6, no. 1, p. 401, Apr 12 2023, doi: 10.1038/s42003-023-04796-0.

[64] A. Di Martino *et al.*, "The autism brain imaging data exchange: towards a large-scale evaluation of the intrinsic brain architecture in autism," *Mol Psychiatry,* vol. 19, no. 6, pp. 659-67, Jun 2014, doi: 10.1038/mp.2013.78.

[65] S. L. Valk, A. Di Martino, M. P. Milham, and B. C. Bernhardt, "Multicenter mapping of structural network alterations in autism," *Hum Brain Mapp,* vol. 36, no. 6, pp. 2364-73, Jun 2015, doi: 10.1002/hbm.22776.

[66] O. Benkarim *et al.*, "Population heterogeneity in clinical cohorts affects the predictive accuracy of brain imaging," *PLoS Biol,* vol. 20, no. 4, p. e3001627, Apr 2022, doi: 10.1371/journal.pbio.3001627.

[67] D. H. Saklofske and M. R. Schoenberg, "Wechsler Adult Intelligence Scale (All Versions)," ed: Springer New York, 2011, pp. 2675-2680.

[68] K. Ankenman, J. Elgin, K. Sullivan, L. Vincent, and R. Bernier, "Nonverbal and verbal cognitive discrepancy profiles in autism spectrum disorders: influence of age and gender," *Am J Intellect Dev Disabil,* vol. 119, no. 1, pp. 84-99, Jan 2014, doi: 10.1352/1944-7558-119.1.84.

[69] A. M. Nader, P. Jelenic, and I. Soulieres, "Discrepancy between WISC-III and WISC-IV Cognitive Profile in Autism Spectrum: What Does It Reveal about Autistic Cognition?," *PLoS One,* vol. 10, no. 12, p. e0144645, 2015, doi: 10.1371/journal.pone.0144645.

[70] S. J. Hong *et al.*, "A convergent structure-function substrate of cognitive imbalances in autism," *Cereb Cortex,* May 12 2022, doi: 10.1093/cercor/bhac156.

[71] B. Fischl, M. I. Sereno, and A. M. Dale, "Cortical surface-based analysis. II: Inflation, flattening, and a surface-based coordinate system," *Neuroimage,* vol. 9, no. 2, pp. 195-207, Feb 1999, doi: 10.1006/nimg.1998.0396.

[72] B. Fischl, M. I. Sereno, R. B. Tootell, and A. M. Dale, "High-resolution intersubject averaging and a coordinate system for the cortical surface," *Hum Brain Mapp,* vol. 8, no. 4, pp. 272-84, 1999, doi: 10.1002/(sici)1097-0193(1999)8:4<272::aid-hbm10>3.0.co;2-4.

[73] A. M. Dale, B. Fischl, and M. I. Sereno, "Cortical surface-based analysis. I. Segmentation and surface reconstruction," *Neuroimage,* vol. 9, no. 2, pp. 179-94, Feb 1999, doi: 10.1006/nimg.1998.0395.

[74] D. S. Marcus *et al.*, "Informatics and data mining tools and strategies for the human connectome project," *Front Neuroinform,* vol. 5, p. 4, 2011, doi: 10.3389/fninf.2011.00004.

[75] D. C. Van Essen, M. F. Glasser, D. L. Dierker, J. Harwell, and T. Coalson, "Parcellations and hemispheric asymmetries of human cerebral cortex analyzed on surface-based atlases," *Cereb Cortex,* vol. 22, no. 10, pp. 2241-62, Oct 2012, doi: 10.1093/cercor/bhr291.

[76] B. Fischl, "FreeSurfer," *Neuroimage,* vol. 62, no. 2, pp. 774-81, Aug 15 2012, doi: 10.1016/j.neuroimage.2012.01.021.

[77] J. L. Stein *et al.*, "Identification of common variants associated with human hippocampal and intracranial volumes," *Nat Genet,* vol. 44, no. 5, pp. 552-61, Apr 15 2012, doi: 10.1038/ng.2250.

[78] S. Sargolzaei *et al.*, "A practical guideline for intracranial volume estimation in patients with Alzheimer's disease," *BMC Bioinformatics,* vol. 16 Suppl 7, no. Suppl 7, p. S8, 2015, doi: 10.1186/1471-2105-16-S7-S8.

[79] C. Craddock *et al.*, "Towards Automated Analysis of Connectomes: The Configurable Pipeline for the Analysis of Connectomes (C-PAC)," *Front. Neuroinform. Conference Abstract: Neuroinformatics 2013,* 2013, doi: 10.3389/conf.fninf.2013.09.00042.

[80] Y. Behzadi, K. Restom, J. Liau, and T. T. Liu, "A component based noise correction method (CompCor) for BOLD and perfusion based fMRI," *Neuroimage,* vol. 37, no. 1, pp. 90-101, Aug 1 2007, doi: 10.1016/j.neuroimage.2007.04.042.

[81] K. Murphy and M. D. Fox, "Towards a consensus regarding global signal regression for resting state functional connectivity MRI," *Neuroimage,* vol. 154, pp. 169-173, Jul 1 2017, doi: 10.1016/j.neuroimage.2016.11.052.

[82] J. P. Fortin *et al.*, "Harmonization of cortical thickness measurements across scanners and sites," *Neuroimage,* vol. 167, pp. 104-120, Feb 15 2018, doi: 10.1016/j.neuroimage.2017.11.024.

[83] W. E. Johnson, C. Li, and A. Rabinovic, "Adjusting batch effects in microarray expression data using empirical Bayes methods," *Biostatistics,* vol. 8, no. 1, pp. 118-27, Jan 2007, doi: 10.1093/biostatistics/kxj037.

[84] J. P. Fortin *et al.*, "Harmonization of multi-site diffusion tensor imaging data," vol. 161, ed: Academic Press Inc., 2017, pp. 149-170.

[85] K. J. Worsley, J. E. Taylor, F. Tomaiuolo, and J. Lerch, "Unified univariate and multivariate random field theory," *Neuroimage,* vol. 23 Suppl 1, pp. S189-95, 2004, doi: 10.1016/j.neuroimage.2004.07.026.

[86] Y. Hochberg and Y. Benjamini, "More powerful procedures for multiple significance testing," *Stat Med,* vol. 9, no. 7, pp. 811-8, Jul 1990, doi: 10.1002/sim.4780090710.

[87] A. F. Alexander-Bloch *et al.*, "On testing for spatial correspondence between maps of human brain structure and function," *Neuroimage,* vol. 178, pp. 540-551, Sep 2018, doi: 10.1016/j.neuroimage.2018.05.070.

[88] C. Paquola, M. R. Bennett, and J. Lagopoulos, "Structural and Functional Connectivity Underlying Gray Matter Covariance: Impact of Developmental Insult," *Brain Connect,* vol. 8, no. 5, pp. 299-310, Jun 2018, doi: 10.1089/brain.2018.0584.

[89] R. Vos de Wael *et al.*, "BrainSpace: a toolbox for the analysis of macroscale gradients in neuroimaging and connectomics datasets," *Commun Biol,* vol. 3, no. 1, p. 103, Mar 5 2020, doi: 10.1038/s42003-020-0794-7.

[90] A. Di Martino *et al.*, "Unraveling the miswired connectome: a developmental perspective," *Neuron,* vol. 83, no. 6, pp. 1335-53, Sep 17 2014, doi: 10.1016/j.neuron.2014.08.050.

[91] N. K. Logothetis and J. Pfeuffer, "On the nature of the BOLD fMRI contrast mechanism," *Magn Reson Imaging,* vol. 22, no. 10, pp. 1517-31, Dec 2004, doi: 10.1016/j.mri.2004.10.018.

[92] S. J. Hong, S. L. Valk, A. Di Martino, M. P. Milham, and B. C. Bernhardt, "Multidimensional Neuroanatomical Subtyping of Autism Spectrum Disorder," *Cereb Cortex,* vol. 28, no. 10, pp. 3578-3588, Oct 1 2018, doi: 10.1093/cercor/bhx229.

[93] C. Ecker *et al.*, "Intrinsic gray-matter connectivity of the brain in adults with autism spectrum disorder," *Proc Natl Acad Sci U S A,* vol. 110, no. 32, pp. 13222-7, Aug 6 2013, doi: 10.1073/pnas.1221880110.

[94] J. D. Power *et al.*, "Functional network organization of the human brain," *Neuron,* vol. 72, no. 4, pp. 665-78, Nov 17 2011, doi: 10.1016/j.neuron.2011.09.006.

[95] C. Paquola *et al.*, "The Unique Cytoarchitecture and Wiring of the Human Default Mode Network," *biorxiv,* 2021, doi: 10.1101/2021.11.22.469533.

[96] S. L. Valk *et al.*, "Shaping brain structure: Genetic and phylogenetic axes of macroscale organization of cortical thickness," *Sci Adv,* vol. 6, no. 39, Sep 2020, doi: 10.1126/sciadv.abb3417.

[97] S. L. Valk *et al.*, "Genetic and phylogenetic uncoupling of structure and function in human transmodal cortex," *Nat Commun,* vol. 13, no. 1, p. 2341, May 9 2022, doi: 10.1038/s41467-022-29886-1.

[98] M. A. Garcia-Cabezas, B. Zikopoulos, and H. Barbas, "The Structural Model: a theory linking connections, plasticity, pathology, development and evolution of the cerebral cortex," *Brain Struct Funct,* vol. 224, no. 3, pp. 985-1008, Apr 2019, doi: 10.1007/s00429-019-01841-9.

[99] Y. J. John, B. Zikopoulos, M. A. Garcia-Cabezas, and H. Barbas, "The cortical spectrum: A robust structural continuum in primate cerebral cortex revealed by histological staining and magnetic resonance imaging," *Front Neuroanat,* vol. 16, p. 897237, 2022, doi: 10.3389/fnana.2022.897237.

[100] J. M. Huntenburg, P.-L. Bazin, and D. S. Margulies, "Large-Scale Gradients in Human Cortical Organization," *Trends in Cognitive Sciences,* vol. 22, no. 1, pp. 21-31, 2018-01-01 2018, doi: 10.1016/j.tics.2017.11.002.

[101] A. Sancha-Velasco, A. Uceda-Heras, and M. A. Garcia-Cabezas, "Cortical type: a conceptual tool for meaningful biological interpretation of high-throughput gene expression data in the human cerebral cortex," *Front Neuroanat,* vol. 17, p. 1187280, 2023, doi: 10.3389/fnana.2023.1187280.

[102] A. P. Bannister, "Inter- and intra-laminar connections of pyramidal cells in the neocortex," *Neurosci Res,* vol. 53, no. 2, pp. 95-103, Oct 2005, doi: 10.1016/j.neures.2005.06.019.

[103] N. Palomero-Gallagher and K. Zilles, "Cortical layers: Cyto-, myelo-, receptor- and synaptic architecture in human cortical areas," *Neuroimage,* vol. 197, pp. 716-741, Aug 15 2019, doi: 10.1016/j.neuroimage.2017.08.035.

[104] M. A. Garcia-Cabezas, H. Barbas, and B. Zikopoulos, "Parallel Development of Chromatin Patterns, Neuron Morphology, and Connections: Potential for Disruption in Autism," *Front Neuroanat,* vol. 12, p. 70, 2018, doi: 10.3389/fnana.2018.00070.

[105] J. Grove *et al.*, "Identification of common genetic risk variants for autism spectrum disorder," *Nat Genet,* vol. 51, no. 3, pp. 431-444, Mar 2019, doi: 10.1038/s41588-019-0344-8.

[106] B. Trost *et al.*, "Genomic architecture of autism from comprehensive whole-genome sequence annotation," *Cell,* vol. 185, no. 23, pp. 4409-4427 e18, Nov 10 2022, doi: 10.1016/j.cell.2022.10.009.

[107] J. J. Hutsler and H. Zhang, "Increased dendritic spine densities on cortical projection neurons in autism spectrum disorders," *Brain Res,* vol. 1309, pp. 83-94, Jan 14 2010, doi: 10.1016/j.brainres.2009.09.120.

[108] D. A. Fair *et al.*, "Development of distinct control networks through segregation and integration," *Proc Natl Acad Sci U S A,* vol. 104, no. 33, pp. 13507-12, Aug 14 2007, doi: 10.1073/pnas.0705843104.

[109] D. A. Fair *et al.*, "Functional brain networks develop from a "local to distributed" organization," *PLoS Comput Biol,* vol. 5, no. 5, p. e1000381, May 2009, doi: 10.1371/journal.pcbi.1000381.

[110] N. U. Dosenbach *et al.*, "Prediction of individual brain maturity using fMRI," *Science,* vol. 329, no. 5997, pp. 1358-61, Sep 10 2010, doi: 10.1126/science.1194144.

[111] M. Ernst, S. Torrisi, N. Balderston, C. Grillon, and E. A. Hale, "fMRI functional connectivity applied to adolescent neurodevelopment," *Annu Rev Clin Psychol,* vol. 11, pp. 361-77, 2015, doi: 10.1146/annurev-clinpsy-032814-112753.

[112] K. Hwang, M. N. Hallquist, and B. Luna, "The development of hub architecture in the human functional brain network," *Cereb Cortex,* vol. 23, no. 10, pp. 2380-93, Oct 2013, doi: 10.1093/cercor/bhs227.

[113] M. S. Thomas, R. Davis, A. Karmiloff-Smith, V. C. Knowland, and T. Charman, "The over-pruning hypothesis of autism," *Dev Sci,* vol. 19, no. 2, pp. 284-305, Mar 2016, doi: 10.1111/desc.12303.

[114] Z. Petanjek, I. Banovac, D. Sedmak, and A. Hladnik, "Dendritic Spines: Synaptogenesis and Synaptic Pruning for the Developmental Organization of Brain Circuits," *Adv Neurobiol,* vol. 34, pp. 143-221, 2023, doi: 10.1007/978-3-031-36159-3_4.

[115] J. M. Kirkland, E. L. Edgar, I. Patel, and A. M. Kopec, "Impaired microglia-mediated synaptic pruning in the nucleus accumbens during adolescence results in persistent dysregulation of familiar, but not novel social interactions in sex-specific ways," *bioRxiv,* May 3 2023, doi: 10.1101/2023.05.02.539115.

[116] L. Wang *et al.*, "Dysfunctional synaptic pruning by microglia correlates with cognitive impairment in sleep-deprived mice: Involvement of CX3CR1 signaling," *Neurobiol Stress,* vol. 25, p. 100553, Jul 2023, doi: 10.1016/j.ynstr.2023.100553.

[117] L. Maliske and P. Kanske, "The Social Connectome - Moving Toward Complexity in the Study of Brain Networks and Their Interactions in Social Cognitive and Affective Neuroscience," *Front Psychiatry,* vol. 13, p. 845492, 2022, doi: 10.3389/fpsyt.2022.845492.

[118] R. C. Paolicelli *et al.*, "Synaptic pruning by microglia is necessary for normal brain development," *Science,* vol. 333, no. 6048, pp. 1456-8, Sep 9 2011, doi: 10.1126/science.1202529.

[119] G. Tang *et al.*, "Loss of mTOR-dependent macroautophagy causes autistic-like synaptic pruning deficits," *Neuron,* vol. 83, no. 5, pp. 1131-43, Sep 3 2014, doi: 10.1016/j.neuron.2014.07.040.

[120] M. Ouyang *et al.*, "Atypical age-dependent effects of autism on white matter microstructure in children of 2-7 years," vol. 37, ed: John Wiley and Sons Inc., 2016, pp. 819-832.

[121] H. J. Kim *et al.*, "Deficient autophagy in microglia impairs synaptic pruning and causes social behavioral defects," *Mol Psychiatry,* vol. 22, no. 11, pp. 1576-1584, Nov 2017, doi: 10.1038/mp.2016.103.

TABLES

Group	ASD	NT
n	103	108
Mean Age (SD) [y]	20.842 (8.112)	19.220 (7.103)
Mean IQ (SD)	104.359 (15.734)	114.176 (12.310)
Mean Verbal IQ (SD)	101.767 (16.823)	113.269 (12.541)
Mean Performance IQ (SD)	105.903 (15.623)	111.833 (12.489)
Mean IQ Ratio (V/Q) (SD)	0.972 (0.167)	1.020 (0.121)
Mean ADOS (SD)	12.612 (3.734)	-
Mean ADOS Communication (SD)	4.243 (1.531)	-
Mean ADOS Social Interaction (SD)	8.369 (2.683)	-
Mean ADOS Repetitive Behavior (SD)	2.029 (1.485)	-

Site	PITT	NYU	USM
n(ASD)/n(NT)	19/20	35/51	49/37
Mean Age (SD) for ASD/NT [y]	20.595 (7.416)/19.618 (6.489)	16.841 (7.536)/17.512 (6.730)	23.795 (7.642)/21.258 (7.479)
Mean ADOS (SD)	12.684 (3.127)	11.286 (4.191)	13.531 (3.373)
Mean ADOS Communication (SD)	4.211 (1.084)	3.629 (1.646)	4.694 (1.461)
Mean ADOS Social Interaction (SD)	8.474 (2.366)	7.657 (2.980)	8.837 (2.511)
Mean ADOS Repetitive Behavior (SD)	2.737 (1.195)	2.057 (1.083)	1.735 (1.741)
Mean IQ (SD) ASD/NT	112.316 (13.634)/110.250 (8.559)	105.286 (13.768)/114.961 (12.091)	100.612 (16.794)/115.216 (14.075)
Mean Verbal IQ (SD) ASD/NT	109.842 (12.208)/108.35 (10.479)	104.171 (14.168)/114.824 (12.106)	96.918 (18.689)/113.784 (13.742)
Mean Performance IQ (SD) ASD/NT	111.263 (14.185)/109.150 (8.015)	105.343 (13.750)/111.608 (13.180)	104.225 (17.171)/113.595 (13.459)
Mean IQ Ratio (V/Q) (SD) ASD/NT	0.999 (0.151)/0.996 (0.099)	0.998 (0.141)/1.039 (0.142)	0.943 (0.188)/1.006 (0.098)

TABLE 1 Study cohort demographic information for ASD and neurotypical control (NT) groups. Age in years (y), SD = standard deviation

	Pearson's r (95% CI)	p
Age	0.151 (0.017 - 0.281)	0.070
ADOS Total	0.047 (-0.148 - 0.238)	0.780
ADOS Communication	0.028 (-0.167 - 0.22)	0.780
ADOS Social Interaction	0.049 (-0.146 - 0.24)	0.780
ADOS Repetitive Behavior	-0.037 (-0.229 - 0.158)	0.780
Full IQ	0.324 (0.197 - 0.44)	**<0.001**
IQ ratio (Verbal/Nonverbal)	0.087 (-0.049 - 0.219)	0.349

Verbal IQ	0.307 (0.18 - 0.425)	**<0.001**
Performance IQ	0.245 (0.114 - 0.368)	**0.001**

TABLE 2 | Correlation between mean CD (CD) in clusters of significant group differences and age, age group (Children <18 years and adults >= 18 years) as well as behavioral metrics. P-values were corrected for multiple comparisons using false discovery rate correction ($q<0.05$). Supplemental Table 1 provides values for each of the twelve clusters separately.